European Journal of Applied Physiology
https://doi.org/10.1007/s00421-025-05974-0

ORIGINAL ARTICLE

Blood flow restriction modulates common drive to motor units and force precision: implications for neuromuscular coordination

Chia-Chan Wu[1] · Yen-Ting Lin[2] · Yueh Chen[3] · Yi-Ching Chen[4,5] · Ing-Shiou Hwang[1,6]

Received: 19 March 2025 / Accepted: 30 August 2025

Abstract

Purpose Blood flow restriction (BFR) is a resistance training technique that enhances muscle adaptation and strength gains under hypoxic conditions. However, its impact on motor unit (MU) coordination remains unclear. This study investigated how BFR influences intra- and inter-muscular common drives to MUs in two functional agonists during a static precision pinch task.

Methods Eighteen adults (23.9 ± 1.3 years; nine men, nine women) performed a thumb–index finger precision pinch under BFR and non-BFR conditions, while force fluctuation dynamics and MU activities in the flexor pollicis brevis (FPB) and first dorsal interosseous (FDI) were analyzed.

Results The results revealed a significant reduction in maximal voluntary contraction following BFR application ($p = 0.003$). In addition, BFR significantly increased force fluctuations ($p = 0.007$), potentiated discharge variability ($p = 0.018$), and strengthened force–discharge coupling specifically in the FPB ($p = 0.010$). BFR increased the mean recruitment threshold of motor units in the FDI ($p < 0.001$), but not in the FPB ($p > 0.05$) during finger precision pinch. Intra-muscular common drive increased within the FDI ($p < 0.001$) and FPB ($p < 0.001$), whereas inter-muscular common drive between agonist MUs decreased ($p < 0.001$).

Conclusion BFR application disrupts force precision stability and neuromuscular coordination between functional agonists during precision pinch. It increases global discharge variability and intra-muscular MU synchrony. However, the resulting force fluctuations are only partially compensated by reduced inter-muscular MU synchrony, offering limited coordination flexibility among agonists.

Keywords Ischemic contraction · Common drive · Motor units · Force fluctuations · EMG

Communicated by Andrew Cresswell .

✉ Ing-Shiou Hwang
ensureh@gmail.com

1 Institute of Allied Health Sciences, College of Medicine, National Cheng-Kung University, Tainan 701, Taiwan

2 Department of Ball Sport, National Taiwan University of Sport, Taichung, Taiwan

3 Orthopedic Department, Kaohsiung Veterans General Hospital Tainan Branch, Tainan, Taiwan

4 Department of Physical Therapy, College of Medical Science and Technology, Chung Shan Medical University, Taichung 40201, Taiwan

5 Physical Therapy Room, Chung Shan Medical University Hospital, Taichung 40201, Taiwan

6 Department of Physical Therapy, College of Medicine, National Cheng Kung University, Tainan 70101, Taiwan

Abbreviations

AI	Artificial intelligence
BFR	Blood flow restriction
BMI	Body mass index
CDI	Common drive index
CDI_{FDI}	Common drive index within first dorsal interosseous
$CDI_{FDI\text{-}FPB}$	Common drive index between first dorsal interosseous and flexor pollicis brevis
CDI_{FPB}	Common drive index within flexor pollicis brevis
DSDC	Decomposition–synthesis–decomposition–compare
EMG	: Electromyography
FDI	First dorsal interosseous
FF_{RMS}	Root mean square of force fluctuations
FF_{SampEn}	Sample entropy of force fluctuations
FPB	Flexor pollicis brevis

Published online: 17 September 2025

MDT	: Mean discharge trace
MDT_{RMS}	Root mean square of mean discharge trace
MI	Mutual information
MU	Motor unit
MUAPT	Motor unit action potential train
MVC	: Maximum voluntary contraction
NBFR	Non-BFR
NO	Nitric oxide
RMS	Root mean square
ROI	Region of interest

Introduction

Blood flow restriction (BFR) is a hypoxic training technique that restricts venous return while maintaining arterial inflow during low-load resistance exercises (Suga et al. 2009; Pope et al. 2013). This approach enhances muscle strength without requiring high loads by limiting oxygen availability, thereby increasing metabolic, and mechanical stress to activate hypertrophic signaling pathways that stimulate muscle protein synthesis (Pearson & Hussain 2015; Biazon et al. 2019). Additionally, BFR-induced release of growth hormone and nitric oxide (NO) promotes vasodilation and nutrient delivery, further supporting muscle growth (Rossi et al. 2018; Christiansen et al. 2019). Studies have demonstrated that low-load BFR training produces muscle growth and strength gains comparable to those of high-load resistance training (Lixandrão et al. 2018; Grønfeldt et al. 2020).

Beyond its effects on muscle adaptation, BFR induces distinct neuromuscular changes, altering motor unit (MU) behaviors. The hypoxic environment promotes early recruitment of high-threshold MUs (type II fibers), which are typically activated only during high-load resistance training (Fatela et al. 2019). BFR applied to the biceps brachii significantly increases MU firing rates, specifically with similarly sized MUs exhibiting higher discharge rates than under non-BFR (NBFR) conditions (Olmos et al. 2024b). However, BFR accelerates muscular fatigue due to hypoxia-induced metabolic stress (Fatela et al. 2016, 2019; Chen et al. 2023; Wu et al. 2024), as evidenced by a faster decline in MU discharge rates compared to NBFR training (Chen et al. 2020; Copithorne et al. 2021; Lowe et al. 2023).

Muscle synergies, defined as coordinated muscle activation patterns, simplify complex force regulation (Berger & d'Avella 2014; Singh et al. 2018). Effective synergies rely on balanced MU coordination within and between muscles, enhancing force stability (Madarshahian et al. 2021) and facilitating adaptation to task complexity. The common drive theory, introduced by De Luca (1982), describes how presynaptic inputs or shared local excitatory interneurons synchronize MU firing patterns. MU coordination can be examined within a single muscle (De Luca & Erim 1994) or between synergistic muscles (De Luca & Erim 2002), typically revealing a short-lag positive correlation in cross-correlation analyses, reflecting shared neural drive. The degree of common drive varies based on task demands, muscle groups, and functional requirements (Laine & Valero-Cuevas 2017; Kenville et al. 2020). Under conditions of fatigue and increased exertion, the common synaptic input to motor neurons intensifies, strengthening MU synchronization (Boonstra et al. 2008; Castronovo et al. 2015; Hwang et al. 2020). Adaptations in common drive following exercise (Ye et al. 2014) and with advancing age (Castronovo et al. 2018) lead to declines in force steadiness because excessive common drive amplifies motor unit synchronization and diminishes motor control precision. Conversely, weaker common synaptic input and greater independence among MUs promote adaptive fatigue responses (Rossato et al. 2022) and flexible muscle coordination (Chen et al. 2019; Rossato et al. 2022). As motor skill proficiency advances, the central nervous system optimizes neuromuscular control by reducing common synaptic input within muscles, prioritizing force precision, and stability (Cabral et al. 2024).

BFR application may alter motor unit (MU) discharge behavior and recruitment patterns, likely through modulation of the central common drive. However, its effects on MU synchrony within and between muscles remain largely unexplored. This study examines how BFR influences force fluctuations, MU behavior, and intra- and inter-muscular common drive in the flexor pollicis brevis (FPB) and first dorsal interosseous (FDI) muscles during a precision pinch task. We hypothesized that 1) BFR would impair force precision control during precision pinch; and 2) BFR would modulate common drive, altering MU discharge patterns and interactions. Elucidating BFR-induced changes in MU synchrony within and between muscles may provide critical insights for optimizing muscle strengthening strategies.

Methods

Subjects

Eighteen healthy young adults (age: 23.9 ± 1.3 years; nine men, nine women; height: 164.6 ± 9.0 cm; weight: 60.4 ± 13.0 kg; BMI: 22.05 ± 3.23 kg/m^2; right-hand dominance) provided informed consent before participating in this study, which was approved by the Institutional Review Board of the National Cheng Kung University Hospital (No. A-ER-112-037). Subjects refrained from vigorous activity and caffeine consumption for 24 h prior to the experiment.

Experimental procedure

On the day of the laboratory visit, the participants first underwent resting blood pressure measurement with an electric sphygmomanometer (HEM-7121; OMRON Inc., Kyoto, Japan). They sat and relaxed for 5 min before their blood pressure was recorded. Next, maximal voluntary contraction (MVC) for finger pinch of the dominant limb was determined. Finger pinch involved pressing the thumb pad against the index finger pad, with the index finger anchored to a force sensor (MB-100, Interface Inc., Scottsdale, USA) mounted on a wooden frame (Fig. 1, left plots). The participants performed three brief (~ 3 s) maximal pinches and the highest value was recorded as the MVC. Following MVC determination, participants completed three trials of a static force-tracking task at 20% MVC, under blood flow restriction (BFR) and non-BFR (NBFR) conditions, to examine motor unit (MU) discharge behaviors during force gradation. A lower exertion level (% MVC) was chosen to ensure that participants could complete all BFR trials. For the static force task, the force trajectory included a 3-s baseline (quiescent) period, a 2-s up-ramp (increasing at 10% MVC/s), a 58-s steady hold at 20% MVC, a 2-s down-ramp (decreasing at 10% MVC/s), and a final 3-s baseline (Fig. 1, right plot). To focus on stable force output, the region of interest (ROI) was defined as 9–58 s of each trial. Muscle activity in the flexor pollicis brevis (FPB) and first dorsal interosseous (FDI) was recorded using 4-pin wireless surface EMG electrodes (Trigno Galileo sensor; Delsys Inc., Natick, MA, USA). Each sensor array (23 × 30 × 7 mm, 19 g) had four active electrodes in a diamond formation with a 5-mm inter-electrode distance.

In the BFR condition, wireless auto-calibrating cuffs (SAGA Fitness, Queensland, Australia) were applied to the biceps brachii muscle belly. Venous return was fully obstructed for 10 min with the restriction pressure set at 80% of systolic blood pressure (104.2 ± 8.8 mmHg) (Wu et al. 2024; Chen et al. 2025). This ischemic preconditioning technique is widely used to enhance upper limb muscle strength under hypoxic conditions. In the NBFR condition, the same setup was used, but restriction pressure was set at 20% of systolic blood pressure. The participants completed three force-tracking trials, separated by 3-min rest intervals, to assess precision pinch force scaling under the BFR and NBFR conditions. The trial order was counterbalanced—half of the participants started with BFR, while the other

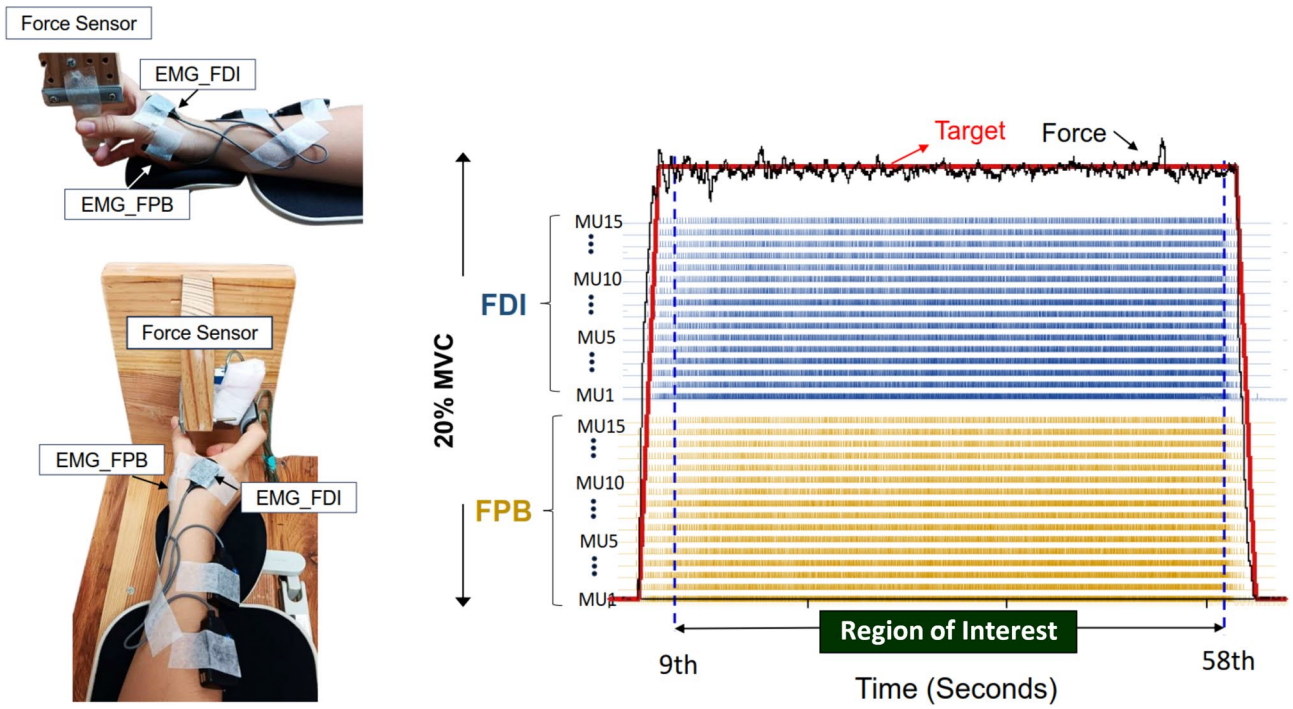

Fig. 1 System setup of precision pinch in this study. The precision pinch task in this study involved pressing the pad of the thumb against the pad of the index finger to scale force according to a target line (left plot). A force sensor was mounted on the wooden frame and the pad of the index finger to monitor force output. Multi-channel surface electromyographic (EMG) arrays were placed on the muscle bellies of the flexor pollicis brevis (FPB) and first dorsal interosseous (FDI). The right plot shows the typical force output, target line for the precision pinch, and decomposition results for the FPB and FDI muscles. The decomposition of multi-channel surface EMG yielded spike trains of motor units, which were labeled as discharge events during the precision pinch task. Only data within the window of interest were considered for further analysis

half began with NBFR. Force data were sampled at 1 kHz via a 16-bit analog-to-digital converter (DAQCard-6024E; National Instruments, Austin, USA) using LabVIEW software. Surface EMG signals were sampled at 2 kHz, band-pass filtered (20–450 Hz), and streamed to EMGworks v.4.7.8 software (Delsys Inc., Natick, USA). Data synchronization between EMG and force recordings was achieved using a common voltage pulse.

Data analysis

Force fluctuations were defined as the force data of finger pinch within the window of interest (9th–58th second) after elimination of its linear trend. The two variables, root mean square (FF_{RMS}), and sample entropy (FF_{SampEn}), represented the force scaling properties of precision pinch. The force fluctuations were down-sampled to 100 Hz before the sample entropy calculation. The mathematical formula of sample entropy was $SampEn(m, r, N) = -\log(\sum_{i=1}^{N-m} A_i / \sum_{i=1}^{N-m} B_i)$, where $r = 20\%$ of the standard deviation of the data, m is the length of the template ($m = 2$), and N is the number of data points in the time series. A_i is the number of matches of the ith template of length $m + 1$ data points, and B_i is the number of matches of the ith template of length m data points. The FF_{RMS} and FF_{SampEn} across three trials were averaged for each participant in the NBFR and BFR conditions.

The surface EMG signals recorded during the entire tracking session in the FDI and FPB muscles were processed using an established AI-based decomposition procedure (De Luca et al. 2006; Nawab et al. 2010; Kline and De Luca 2014) to obtain motor unit (MU) spike trains with NeuroMap v.1.2.1 (Delsys Inc., Natick, MA, USA). The validity of the EMG decomposition results of each MUAPT was evaluated with the Decomposition–Synthesis–Decomposition–Compare (DSDC) test. Only MUs with a decomposition accuracy exceeding 85% using the DSDC method were included for further analysis. Discharge events of the decomposed MUs were identified during the experimental trials and only the spike trains of MUs within the window of interest were considered for further analysis. In this study, we focused on analyzing the low-frequency common drive to the MUs of the FDI and FPB muscles by estimating the cumulative spike trains of all identified motor units, followed by smoothing and averaging processes (Fig. 2). The cumulative spike trains in the window of interest were smoothed by convolution with a Hanning window (duration: 400 ms) (Negro and Farina 2012). The smoothed discharge trace was normalized by the number of

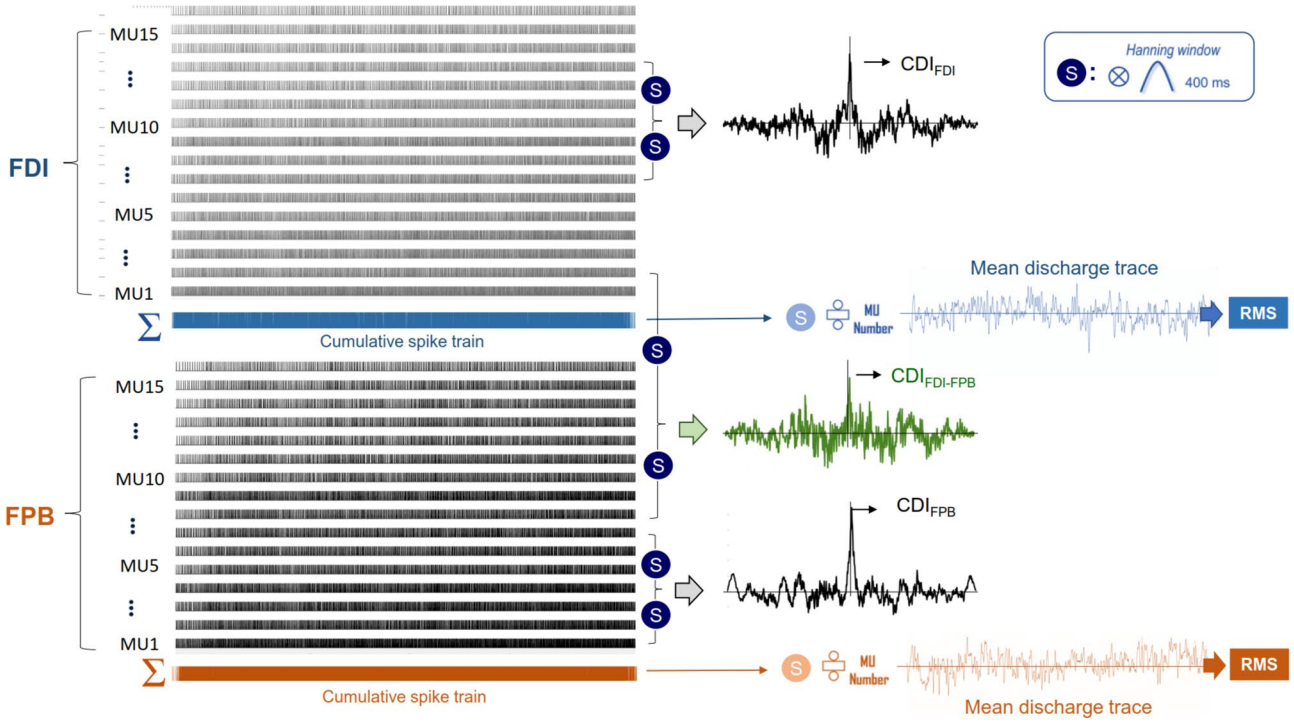

Fig. 2 Schematic illustration of signal processing for common drive index within the first dorsal interosseous (CDI_{FDI}), within the flexor pollicis brevis (CDI_{FPB}), and between the FDI and FPB ($CDI_{FDI\text{-}FPB}$). The surface EMG from two muscles was decomposed into motor unit spike trains. The summation of these spike trains resulted in a cumulative motor unit spike train, which was then smoothed into a mean discharge trace (MDT) by convolving it with a 400-ms Hanning window (the smoothing process) and dividing by the number of decomposed motor units. The size of fluctuations in the MDT was indexed using the root mean square (RMS) of the MDT after the removal of its linear trend. The circle S denotes the smoothing process of a motor unit spike train

active motor units to obtain the mean discharge trace (MDT) for each experimental trial. The variability of the pooled discharges from MUs (MDT_{RMS}) was estimated by applying the RMS to the MDT after the removal of the linear trend. The RMS of the MDT from the three experimental trials for both the FDI and FPB muscles was averaged for each participant. Due to the non-linear properties associated with the viscous resistance of the musculotendon system, the degree of discharge-force coupling was characterized using entropy-based mutual information (MI) (Hwang et al. 2017, 2020). Mutual information ($MI(X;Y)$) was defined as: $MI(X;Y) = \sum_{y\in Y}\sum_{x\in X} p(x,y)\log(p(x,y)/p_1(x)p_2(y))$, where $p(x,y)$ is the joint probability density function of force fluctuations (X) and detrended mean discharge rate trace (Y), and $p_1(x)$ and $p_2(y)$ are the marginal probability density functions of the two time series, respectively. A higher MI indicates that the variability of pooled discharges better accounts for the force fluctuations during precision pinch.

In addition, we calculated the traditional common drive index (CDI) within and between the FDI and FPB muscles (De Luca and Erim 1994, 2002). The calculation involved a smoothing procedure by convolution of the motor unit spike train of each MU with a 400-ms Hanning window (Fig. 2). For an experimental trial, the cross-correlation plot ($\widetilde{R}_{xy}$) was calculated for the smoothed discharge trace from a given MU pair: $\widetilde{R}_{xy} = \frac{r_{xy}(t,\tau)}{\sqrt{r_{xx}(t,0)r_{yy}(t,0)}}$, where $r_{xy}(t,\tau) = x\left(t+\frac{\tau}{2}\right)y\left(t-\frac{\tau}{2}\right)$, x and y are smoothed discharge traces of the two considered motor units, t is the time variable, and τ is the time-lag variable. The correlation plot ($\widetilde{R}_{xy}$) was further remapped to a normalized correlation plot with Fisher z transformation ($z = \frac{1}{2}ln\left(\frac{1+\widetilde{R}_{xy}}{1-\widetilde{R}_{xy}}\right)$) (Chen et al. 2019). If a motor unit pair was composed of two MUs of a muscle (FDI or FPB), the maxima represented CDI within the muscle (CDI_{FDI} or CDI_{FPB}). If a motor unit pair consisted of two MUs from different muscles, the maxima of $\widetilde{R}_{xy}$ represented the common drive index between the muscles ($CDI_{FDI\text{-}FPB}$).

Statistical analysis

On an individual basis, a multivariate Hotelling's T^2 test, followed by post-hoc paired t-tests, was used to assess differences in force fluctuation variables (FF_{RMS} and FF_{SampEn}) between the NBFR and BFR conditions. Similarly, Hotelling's T^2 test and post-hoc paired t-tests were applied to compare MDT RMS and discharge-force coupling for the FDI and FPB muscles between conditions. Recruitment thresholds of pooled motor units during finger precision pinch in the NBFR and BFR conditions were compared using a permutation paired t-test. For CDI_{FDI}, CDI_{FPB}, and $CDI_{FDI\text{-}FPB}$, a permutation paired t-test was conducted to compare the mean CDI values of all motor unit pairs across participants in the NBFR and BFR conditions. The number of permutation for all tests was 10,000. All data are reported as group means ± 1 standard deviation. Statistical analyses were performed in IBM SPSS Statistics (v19), with significance set at $\alpha = 0.05$.

Results

The maximal voluntary contraction (MVC) of finger pinch before and after BFR application was 50.18 ± 27.44 N and 43.32 ± 24.89 N, respectively, reflecting an average reduction of 13.65 ± 18.16% following BFR application. A paired t test revealed a significant reduction in MVC under the BFR condition compared to the NBFR condition ($t_{17} = 3.414$, $p = 0.003$). The size and complexity of force fluctuations under the NBFR and BFR conditions were assessed using RMS (FF_{RMS}) and sample entropy (FF_{SampEn}). Hotelling's T^2 test revealed a significant effect of BFR on force fluctuation metrics ($\Lambda = 0.573$, $p = 0.012$) (Table 1). Post-hoc analysis showed that FF_{RMS} was significantly larger under BFR than under NBFR ($p = 0.007$), while FF_{SampEn} did not differ significantly ($p = 0.117$).

In total, we analyzed 745 motor units (NBFR) and 845 motor units (BFR) in the FDI muscle, and 594 (NBFR) and 751 (BFR) in the FPB muscle. On average, the number of decomposed motor units per trial in the FDI muscle was 13.8 ± 4.7 (NBFR) and 15.7 ± 5.4 (BFR), while in the FPB muscle it was 11.0 ± 4.9 (NBFR) and 13.9 ± 4.8 (BFR). Figure 3a presents a mean discharge trace RMS (MDT_{RMS}) for

Table 1 The contrast of root mean square (FF_{RMS}) and sample entropy (FF_{SampEn}) of force fluctuations between the non-BFR and BFR conditions for submaximal wrist extension and finger opposition. (*: BFR > NBFR, $p < .05$)

	NBFR	BFR	*Post-hoc test*
FF_{RMS} (%MVC)	**0.341 ± 0.102**	**0.399 ± 0.126**	**$t_{17} = -3.081$, $p = 0.007$**
FF_{SampEn}	0.244 ± 0.047	0.254 ± 0.046	$t_{17} = -1.650$, $p = 0.117$
Hotelling's T^2 Statistics	**$\Lambda = 0.573$, $p = 0.012$**		

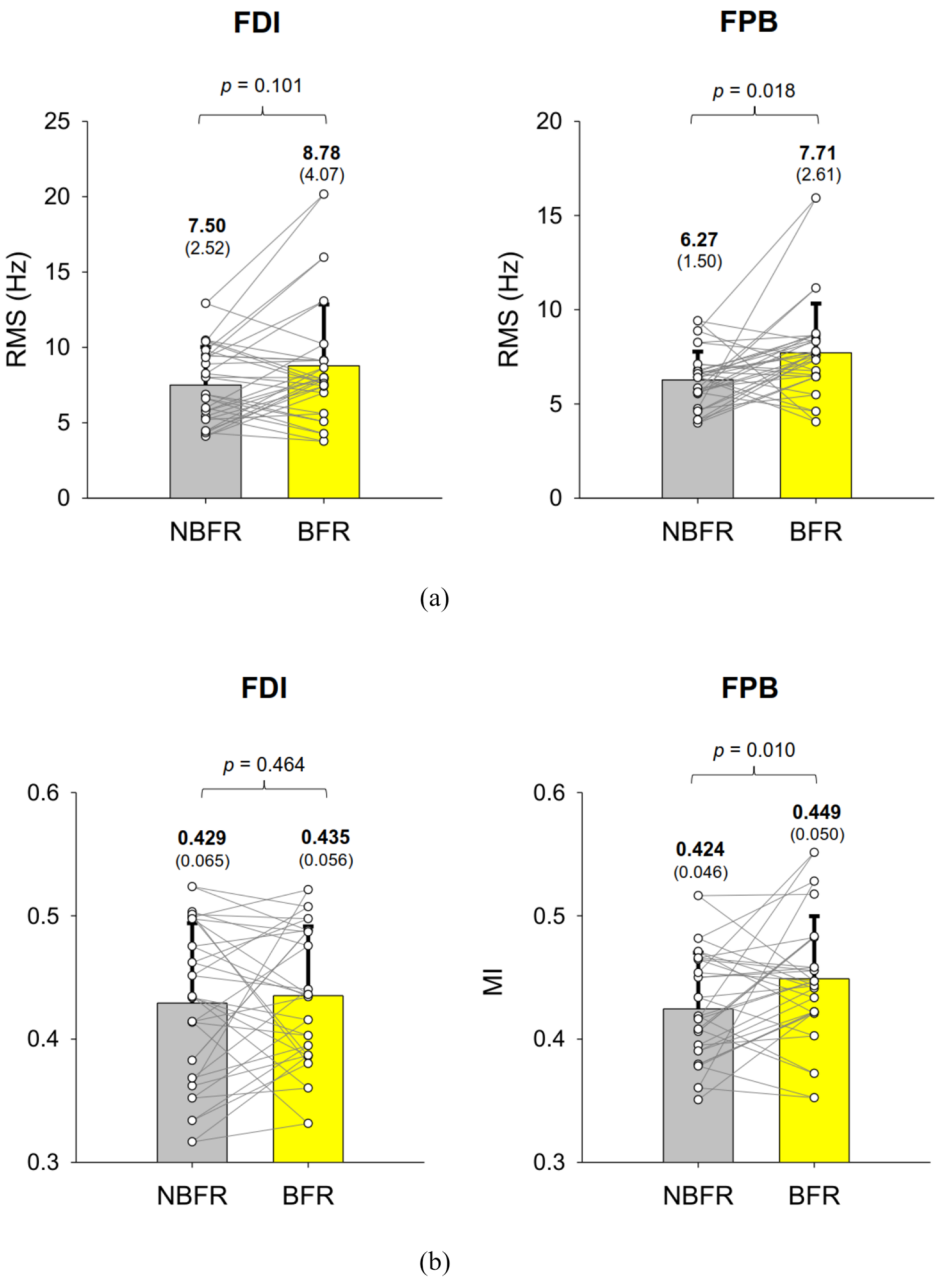

Fig. 3 **A** Comparison of the size of fluctuations in the mean discharge trace (MDT) of the FDI and FPB muscles between the NBFR and BFR conditions. **B** Comparison of the mutual information (MI) between the discharge fluctuations of the MDT and force fluctuations of the FDI and FPB muscles between the NBFR and BFR conditions. The comparison was based on the population means of the variables for each participant (n = 18). *BFR* blood flow restriction, *NBFR* non-blood flow restriction

the FDI and FPB muscles under BFR and NBFR conditions. Hotelling's T^2 test indicated that MDT_{RMS} varied significantly between conditions ($\Lambda = 0.629$, $p = 0.022$). Post-hoc analysis revealed that MDT_{RMS} was significantly greater in the FPB muscle under BFR ($t_{17} = -2.620$, $p = 0.018$). However, while MDT_{RMS} of the FDI muscle tended to increase with BFR, the difference did not reach significance ($t_{17} = -1.735$, $p = 0.101$). Figure 3b illustrates mutual information (MI) between MDT of the FDI/FPB muscles and force fluctuations. Hotelling's T^2 test confirmed that MI varied significantly between conditions ($\Lambda = 0.630$, $p = 0.025$). Post-hoc tests showed that, while MI for FDI MDT and force fluctuations did not differ significantly between conditions ($t_{17} = -0.748$, $p = 0.464$), MI for FPB MDT and force fluctuations was significantly potentiated under BFR ($t_{17} = -2.884$, $p = 0.010$).

Figure 4 shows the contrast of recruitment threshold of MUs in the FDI and FPB between the NBFR and BFR conditions. The results of permutation t test revealed that recruitment thresholds of MU in the FDI in the BFR condition (4.07 ± 4.14%MVC) was larger than that in the NBFR conditions (3.04 ± 3.45%MVC) ($p < 0.001$). However, no significant difference in recruitment threshold of MU in the FPB between NBFR and BFR conditions (NBFR: 4.92 ± 5.67%MVC; BFR: 4.72 ± 5.44%MVC) ($p = 0.196$). Figure 5 (left plots) displays the histograms of common

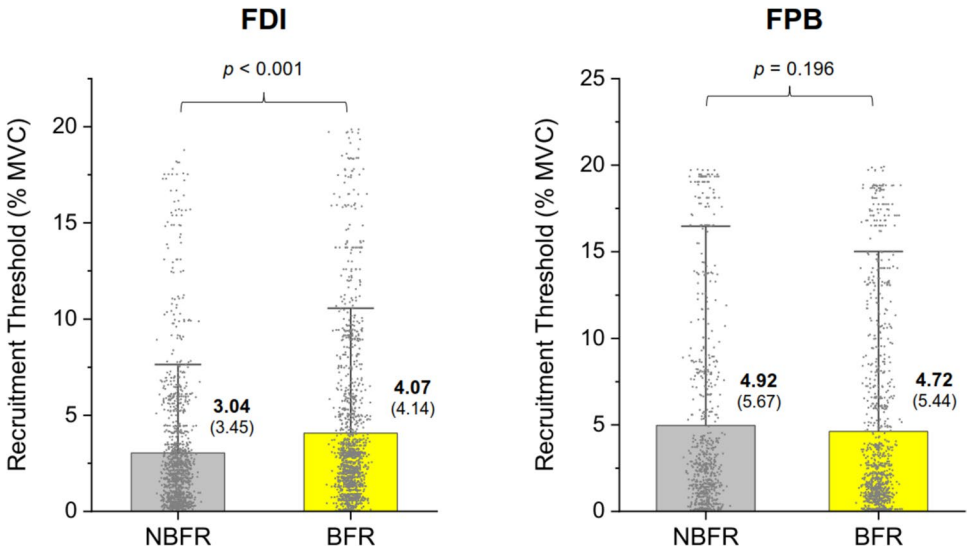

Fig. 4 The figure contrasts the distribution and mean recruitment thresholds of pooled motor units in the FDI and FPB muscles under NBFR and BFR conditions. Each dark gray dot represents the recruitment threshold of an individual motor unit

drive indices (CDI) within (CDI_{FDI} and CDI_{FPB}) and between ($CDI_{FDI\text{-}FPB}$) all motor unit pairs in the FDI and FPB muscles under the NBFR and BFR conditions. Permutation paired t-tests revealed significant differences in CDI_{FDI}, CDI_{FPB}, and $CDI_{FDI\text{-}FPB}$ between conditions ($p < 0.001$) (Fig. 4, right plots). CDI_{FDI} and CDI_{FPB} increased under BFR as compared to under NBFR. In contrast, $CDI_{FDI\text{-}FPB}$ decreased under BFR, with a notable percentage increase in negative $CDI_{FDI\text{-}FPB}$ values, indicating greater inter-muscular independence.

Discussion

This study demonstrated that blood flow restriction (BFR) modulated force control, motor unit (MU) discharge patterns, and MU synchrony within and between agonist muscles. Specifically, BFR reduced force generation capacity and increased force fluctuations (FF_{RMS}) during finger pinch, accompanied by heightened discharge variability and stronger force–discharge coupling in the FPB. Recruitment threshold of FDI was higher in the BFR condition during finger precision pinch. Additionally, intra-muscular common drive (CDI_{FDI} and CDI_{FPB}) increased, while inter-muscular common drive ($CDI_{FDI–FPB}$) decreased, which indicated enhanced intra-muscular synchrony but greater functional independence between agonist muscles following BFR application.

Variations in force characteristics and MU discharge pattern

The slight reduction in MVC following BFR application ($-13.65 \pm 18.16\%$) is consistent with the findings reported by Yasuda et al. (2009). Passive BFR without concurrent exercise may impair force generation capacity before finger precision pinch, likely due to accelerated metabolite accumulation (e.g., lactate and H^+) (Pope et al. 2013; Pearson & Hussain 2015), which can disrupt cross-bridge cycling and induce central inhibition via group III/IV afferents (Gandevia 2001). However, this fatigue-like response differs from fatigue response seen after prolonged submaximal contractions. Unlike true mechanical fatigue caused by sustained activation and metabolic depletion, passive BFR does not overload MUs particularly for low-threshold MUs. In addition, transient reductions in tissue blood flow have been shown to increase local muscle stiffness (Kimura et al. 2007), in contrast to the increased intramuscular compliance typically observed following sustained muscle contraction (García-Manso et al. 2011). Given the observed decline in force generation capacity, passive BFR is expected to influence subsequent force-scaling strategies, in consequence to neuromuscular adaptations in MU recruitment patterns and/or synergies within and between synergist muscles.

BFR application impaired force steadiness, as reflected by increased FF_{RMS} compared to that of NBFR (Table 1). This decline may stem from disrupted calcium handling during excitation–contraction coupling, driven by lactate accumulation under hypoxic conditions (Husmann et al. 2018). From a MU perspective, BFR-induced earlier recruitment of higher-threshold MUs contributes to unsmooth twitch-force fusion and force instability (Fatela et al. 2019), given the larger, shorter-duration twitch forces and lower discharge rates of these recruited MUs. Centrally, BFR may impair corticospinal adaptation to fatigue due to lower levels of cerebral oxygenation (Peyrard et al. 2019; Zambolin et al. 2024). Peripherally, decomposition surface EMG studies report increased MU firing rates (Fatela et al. 2019; Olmos et al. 2024b) and greater discharge variability with BFR (Lowe et al. 2023), resembling the discharge patterns observed in

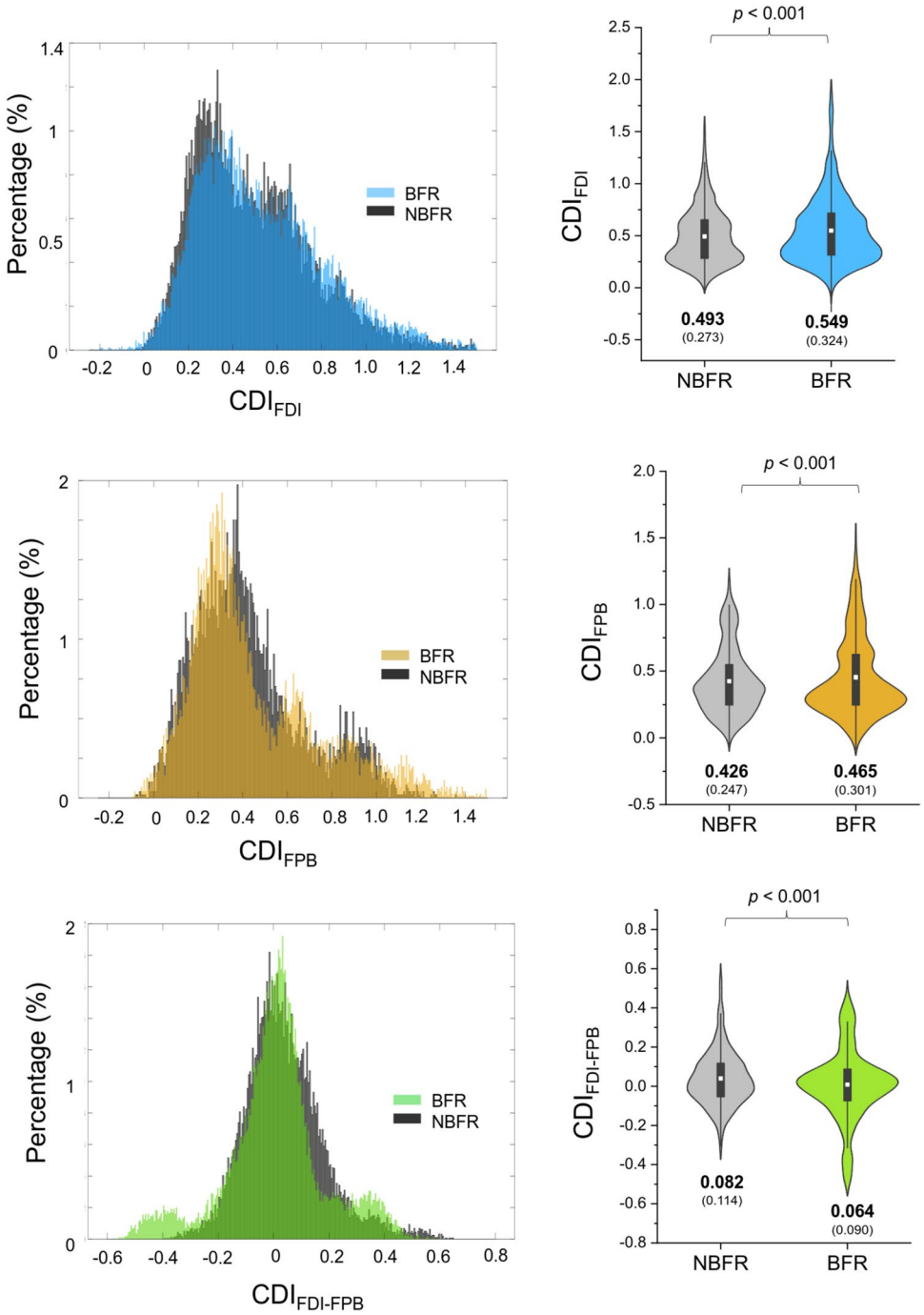

Fig. 5 The contrasts of histograms and means of intra-muscular (CDI_{FDI} and CDI_{FPB}) and inter-muscular ($CDI_{FDI\text{-}FPB}$) common drive between the FDI and FPB muscles in the NBFR and BFR conditions. The comparison was based on the pooled CDI_{FDI}, CDI_{FPB}, and $CDI_{FDI\text{-}FPB}$ from all motor unit pairs across subjects. *BFR* blood flow restriction, *NBFR* non-blood flow restriction, *FPB* flexor pollicis brevis, *FDI* first dorsal interosseous

peripheral neuromuscular fatigue. In line with existing evidence on BFR's central and peripheral effects, our study revealed a pronounced increase in MU discharge variability (MDT_{RMS}) in the FPB muscle during finger pinch (Fig. 3a), underscoring its selective impact on agonist muscle control and force stability. MDT_{RMS} reflects fluctuations in low-frequency common neural inputs (0–4 Hz), correlating with voluntary force output variability (Negro & Farina 2011; Farina & Negro 2015). Under fatigue conditions, increased low-frequency common input leads to greater MU discharge variability and reduces force steadiness (Hwang et al. 2020). By analogy, the increased MDT_{RMS} in BFR trials accounts for the observed force fluctuations during precision pinch. This interpretation is further reinforced by the elevated force-discharge coupling (MI) in the FPB muscle (Fig. 3b), suggesting that MU discharge fluctuations directly contribute to force instability through the musculo-tendon system's low-pass filtering dynamics. Both the FPB and FDI are primary agonists in precision pinch (Long et al. 1970; Lee et al. 2012). However, given that the maximal strength of the FPB

exceeds that of the FDI (Chen et al. 2018), precision pinch force steadiness under BFR appears to depend more on FPB stability. This reliance is particularly evident when the FDI's force contribution is lower, as in the relatively neutral pinching position used in this study (Zijdewind et al. 1998). However, the selective susceptibility of these agonist muscles to ischemic contraction remains an open question, warranting further investigation.

Variations in intra-muscular and inter-muscular MU synchrony

Previous studies reported that BFR could accelerate higher-threshold MU recruitment during the steady force-segment (Fatela et al. 2019; Olmos et al. 2024a). This observation aligns with our current finding of an increased mean recruitment threshold of MUs in the FDI during finger precision pinch under the BFR condition (Fig. 4). However, recruitment threshold of MUs in the FPB did not significantly vary with BFR application. The selective response is likely due to anatomical and hemodynamic differences between the radial and ulnar arteries following upper limb BFR (Loenneke et al. 2013; Condello et al. 2022). The superficial radial artery, which supplies the FDI, is more susceptible to cuff occlusion pressure, whereas the ulnar artery, supplying the FPB, may remain partially perfused. This selective BFR-related response between the FDI and FPB has not been previously reported, motivating further exploration of MU synergy variations between the two muscles.

Compared to the NBFR condition, intra-muscular MU synchrony, indicated by mean CDI_{FDI} and CDI_{FPB}, was elevated under BFR (Fig. 4, upper and middle). The present findings are congruent with previous findings of increased common synaptic input within a muscle during fatigue (Contessa et al. 2009; Castronovo et al. 2015; McManus et al. 2016) and heightened cognitive load (Kitatani et al. 2023). Given the greater fatigue susceptibility under BFR, this rise in intra-muscular synchrony may serve as a compensatory strategy to sustain force output as contractile efficiency declines with BFR-induced fatigue. However, this adaptation could physically contribute to jerky force production, as MUs fire in clusters rather than in a staggered pattern, leading to in-phase twitch forces. In contrast, inter-muscular MU synchrony ($CDI_{FDI\text{-}FPB}$) significantly decreased under BFR (Fig. 4, lower right). This decline is ascribed to an increased proportion of MU pairs exhibiting negative CDI values, as shown in the $CDI_{FDI\text{-}FPB}$ histogram (Fig. 4, lower left). Reduced inter-muscular synchrony has been reported between the FDI and FDS during precision pinch (Laine & Valero-Cuevas 2017) and in fatigue studies (Watanabe et al. 2018; Rossato et al. 2022). Functionally, this reduction enhances the degrees of freedom in muscle coordination, promoting more flexible and adaptive agonist control (Rossato et al. 2022). Functionally, out-of-phase twitch force summation between MU pairs of the two agonists may counteract excessive force fluctuations caused by heightened intra-muscular synchrony due to BFR. The exact mechanisms driving the hypoxia-induced reduction in inter-muscular MU synchrony remain unclear. One possibility is that hypoxia-induced fatigue increases synaptic noises in the neural drive (Jones et al. 2002), weakening the common oscillatory signals shared between muscles. Additionally, metabolic stress-related alterations in proprioceptive signaling (including Ia, Ib, and Group III/IV afferents) may disrupt muscle synergy (Windhorst et al. 2007), further contributing to impaired coordination. Finally, BFR led to increased recruitment heterogeneity due to the activation of high-threshold motor units in the FDI (Fig. 4). In the BFR condition, the CDI between higher-threshold FDI motor units and lower-threshold FPB motor units may be lower than the CDI observed between motor units with similar thresholds under NBFR.

Methodological considerations

This study warrants consideration of several methodological aspects: (1) Motor unit tracking limitations: although EMG electrode positioning was consistent, identical MUs may not have been tracked across the BFR and NBFR conditions due to variations in decomposition. However, this bias was largely minimized by analyzing a pooled set of MUs; (2) Surface EMG decomposition issues: the decomposition algorithms and system for surface EMG signals remain a topic of debate, with no consensus reached on their accuracy and validity (Farina et al. 2011; De Luca et al. 2015). Resolving these longstanding methodological disputes is beyond the scope of this study, and both decomposition approaches are currently accepted for research purposes. We used few-channel recordings with Delsys 5-pin sensors to analyze motor unit activities in the thenar and hypothenar muscles for practical convenience. Moreover, as the study did not require high spatial resolution of motor units, typically favored by high-density electrodes, this method was well-suited to our research objectives. (3) Limited muscle selection: this study focused on two specific agonist muscles (FPB and FDI) in a precision pinch task. However, MU synchrony modulation may vary depending on task demands (Laine & Valero-Cuevas 2017), muscle-specific characteristics (Hug et al. 2021), and individual differences (Avrillon et al. 2021). For example, the present findings on motor unit synergy differ from those of Chen et al. (2025), where combined BFR and neuromuscular stimulation modulated synergy between ECRL and ECRB. Beyond differences in innervation, the ECRB–ECRL pair functions as a unidirectional force couple for wrist extension, supporting gross motor synergy for force generation and stabilization. In

contrast, the FDI–FPB pair produces opposing directional pulls across the palmar space, facilitating fine motor synergy essential for dexterity and precision. The origin of fatigue responses in Chen et al. (2025) also differed from the present study. Modulation of motor unit synergy may vary between combined BFR with neuromuscular stimulation and BFR alone. Given these factors, caution is advised when generalizing these findings, and further research is needed to validate and expand upon these observations.

Conclusion

This study unveils novel evidence that blood flow restriction modulates neuromuscular control within functional agonists, amplifying global discharge variability and MU synchrony within a muscle while diminishing synchrony between muscles. These neurophysiological alterations likely underlie the observed decline in force steadiness with BFR. Notably, whether neuromuscular coordination adapts differently following low-load BFR resistance training compared to traditional resistance training, despite comparable strength gains, remains an open question.

Author contributions C.C.W., Y.C., Y.C.C., and I.S.H. designed the experiments. C.C.W. conducted the experiments. C.C.W. and Y.T.L. analyzed the data. C.C.W. and I.S.H. wrote the paper. Y.C.C. and I.S.H. securing funding. I.S.H. provided final approval. All authors read and approved the manuscript.

Funding This research was supported by grants from the National Science and Technology Council, Taiwan, R.O.C., under Grants No. NSTC 112–2410-H-040–004- and NSTC 111–2314-B-006 -062 -MY3).

Data avilability The raw data generated for this study are not publicly available in order to protect participants' privacy, but the sample data are available from the corresponding author upon reasonable request.

Declarations

Conflict of interest The authors declare that they have no conflicts of interest.

Ethical approval All procedures performed in studies involving human participants were in accordance with the ethical standards of the institutional and/or national research committee (Institutional Review Board (IRB) at the National Cheng Kung University (NCKU) Hospital, Taiwan, No. A-ER-112–037) and with the 1964 Helsinki declaration and its later amendments or comparable ethical standards.

References

Avrillon S, Del Vecchio A, Farina D et al (2021) Individual differences in the neural strategies to control the lateral and medial head of the quadriceps during a mechanically constrained task. J Appl Physiol 130:269–281. https://doi.org/10.1152/japplphysiol.00653.2020

Berger DJ, d'Avella A (2014) Effective force control by muscle synergies. Front Comput Neurosci 8:46. https://doi.org/10.3389/fncom.2014.00046

Biazon TMPC, Ugrinowitsch C, Soligon SD et al (2019) The association between muscle deoxygenation and muscle hypertrophy to blood flow restricted training performed at high and low loads. Front Physiol 10:446. https://doi.org/10.3389/fphys.2019.00446

Boonstra TW, Daffertshofer A, van Ditshuizen JC et al (2008) Fatigue-related changes in motor-unit synchronization of quadriceps muscles within and across legs. J Electromyogr Kinesiol 18:717–731. https://doi.org/10.1016/j.jelekin.2007.03.005

Cabral HV, Cudicio A, Bonardi A et al (2024) Neural filtering of physiological tremor oscillations to spinal motor neurons mediates short-term acquisition of a skill learning task. eNeuro 11:ENEURO.0043-24.2024. https://doi.org/10.1523/ENEURO.0043-24.2024

Castronovo AM, Negro F, Conforto S et al (2015) The proportion of common synaptic input to motor neurons increases with an increase in net excitatory input. J Appl Physiol 119:1337–1346. https://doi.org/10.1152/japplphysiol.00255.2015

Castronovo AM, Mrachacz-Kersting N, Stevenson AJT et al (2018) Decrease in force steadiness with aging is associated with increased power of the common but not independent input to motor neurons. J Neurophysiol 120:1616–1624. https://doi.org/10.1152/jn.00093.2018

Chen CY, McGee CW, Rich TL et al (2018) Reference values of intrinsic muscle strength of the hand of adolescents and young adults. J Hand Ther 31:348–356. https://doi.org/10.1016/j.jht.2017.05.012

Chen YC, Shih CL, Lin YT et al (2019) The effect of visuospatial resolution on discharge variability among motor units and force-discharge relation. Chin J Physiol 62:166–174. https://doi.org/10.4103/CJP.CJP_12_19

Chen YC, Su YH, Lin YT et al (2020) Acute physiological responses to combined blood flow restriction and low-level laser. Eur J Appl Physiol 120:1437–1447. https://doi.org/10.1007/s00421-020-04378-6

Chen YC, Lin YT, Hu CL et al (2023) Low-level laser therapy facilitates postcontraction recovery with ischemic preconditioning. Med Sci Sports Exerc 55:1326–1333. https://doi.org/10.1249/MSS.0000000000003149

Chen YC, Wu CC, Lin YT et al (2025) Adaptive modification in agonistcommon drive after Combined blood flow restriction and neuromuscular electrical stimulation. IEEE Trans Neural Syst Rehabil Eng. https://doi.org/10.1109/TNSRE.2025.3525517

Christiansen D, Eibye KH, Rasmussen V et al (2019) Cycling with blood flow restriction improves performance and muscle K+ regulation and alters the effect of antioxidant infusion in humans. J Physiol 597:2421–2444. https://doi.org/10.1113/JP277657

Condello F, Cacia M, Sturla M et al (2022) Simultaneous radial and ipsilateral ulnar artery compression versus isolated radial artery compression after conventional radial access for coronary angiography and/or intervention: a systematic review and meta-analysis. J Clin Med 11(23):7013. https://doi.org/10.3390/jcm11237013

Contessa P, Adam A, De Luca CJ (2009) Motor unit control and force fluctuation during fatigue. J Appl Physiol 107:235–243. https://doi.org/10.1152/japplphysiol.00035.2009

Copithorne DB, Hali K, Rice CL (2021) The effect of blood flow on tibialis anterior motor unit firing rates during sustained low-intensity isometric contractions. Appl Physiol Nutr Metab 46:63–68. https://doi.org/10.1139/apnm-2020-0437

De Luca CJ, Erim Z (1994) Common drive of motor units in regulation of muscle force. Trends Neurosci 17:299–305. https://doi.org/10.1016/0166-2236(94)90064-7

De Luca CJ, Erim Z (2002) Common drive in motor units of a synergistic muscle pair. J Neurophysiol 87:2200–2204. https://doi.org/10.1152/jn.00793.2001

De Luca CJ, LeFever RS, McCue MP et al (1982) Control scheme governing concurrently active human motor units during voluntary contractions. J Physiol 329:129–142. https://doi.org/10.1113/jphysiol.1982.sp014294

De Luca CJ, Adam A, Wotiz R et al (2006) Decomposition of surface EMG signals. J Neurophysiol 96:1646–1657. https://doi.org/10.1152/jn.00009.2006

De Luca CJ, Nawab SH, Kline JC (2015) Clarification of methods used to validate surface EMG decomposition algorithms as described by Farina et al. (2014). J Appl Physiol 118:1084. https://doi.org/10.1152/japplphysiol.00061.2015

Farina D, Enoka RM (2011) Surface EMG decomposition requires an appropriate validation. J Neurophysiol 105:981–982. https://doi.org/10.1152/jn.00855.2010

Farina D, Negro F (2015) Common synaptic input to motor neurons, motor unit synchronization, and force control. Exerc Sport Sci Rev 43:23–33. https://doi.org/10.1249/JES.0000000000000032

Fatela P, Reis JF, Mendonca GV et al (2016) Acute effects of exercise under different levels of blood-flow restriction on muscle activation and fatigue. Eur J Appl Physiol 116:985–995. https://doi.org/10.1007/s00421-016-3359-1

Fatela P, Mendonca G, Veloso A et al (2019) Blood flow restriction alters motor unit behavior during resistance exercise. Int J Sports Med 40:555–562. https://doi.org/10.1055/a-0888-8816

Gandevia SC (2001) Spinal and supraspinal factors in human muscle fatigue. Physiol Rev 81(4):1725–1789. https://doi.org/10.1152/physrev.2001.81.4.1725

García-Manso JM, Rodríguez-Ruiz D, Rodríguez-Matoso D, de Saa Y, Sarmiento S, Quiroga M (2011) Assessment of muscle fatigue after an ultra-endurance triathlon using tensiomyography (TMG). J Sports Sci 29(6):619–625. https://doi.org/10.1080/02640414.2010.548822

Grønfeldt BM, Lindberg Nielsen J, Mieritz RM et al (2020) Effect of blood-flow restricted vs heavy-load strength training on muscle strength: systematic review and meta-analysis. Scand J Med Sci Sports 30:837–848. https://doi.org/10.1111/sms.13632

Hug F, Del Vecchio A, Avrillon S et al (2021) Muscles from the same muscle group do not necessarily share common drive: evidence from the human triceps surae. J Appl Physiol 130:342–354. https://doi.org/10.1152/japplphysiol.00635.2020

Husmann F, Mittlmeier T, Bruhn S et al (2018) Impact of blood flow restriction exercise on muscle fatigue development and recovery. Med Sci Sports Exerc 50:436–446. https://doi.org/10.1249/MSS.0000000000001475

Hwang IS, Lin YT, Huang WM et al (2017) Alterations in neural control of constant isometric contraction with the size of error feedback. PLoS ONE 12:e0170824. https://doi.org/10.1371/journal.pone.0170824

Hwang IS, Lin YT, Huang CC et al (2020) Fatigue-related modulation of low-frequency common drive to motor units. Eur J Appl Physiol 120:1305–1317. https://doi.org/10.1007/s00421-020-04363-z

Jones KE, Hamilton AF, Wolpert DM (2002) Sources of signal-dependent noise during isometric force production. J Neurophysiol 88:1533–1544. https://doi.org/10.1152/jn.2002.88.3.1533

Kenville R, Maudrich T, Vidaurre C et al (2020) Intermuscular coherence between homologous muscles during dynamic and static movement periods of bipedal squatting. J Neurophysiol 124:1045–1055. https://doi.org/10.1152/jn.00231.2020

Kimura K, Watanabe Y, Umeda M et al (2007) Quantitative analysis of the relation between soft tissue stiffness palpated from the body surface and tissue hemodynamics in the human forearm. Physiol Meas 28(12):1495–1505. https://doi.org/10.1088/0967-3334/28/12/004

Kitatani R, Furukawa K, Sakaue D et al (2023) Influences of different cognitive loads on central common neural drives to the ankle muscles during dual-task walking. Neurosci Lett 804:137214. https://doi.org/10.1016/j.neulet.2023.137214

Kline JC, De Luca CJ (2014) Error reduction in EMG signal decomposition. J Neurophysiol 112:2718–2728. https://doi.org/10.1152/jn.00724.2013

Laine CM, Valero-Cuevas FJ (2017) Intermuscular coherence reflects functional coordination. J Neurophysiol 118:1775–1783. https://doi.org/10.1152/jn.00204.2017

Lee SK, Wisser JR (2012) Restoration of pinch in intrinsic muscles of the hand. Hand Clin 28:45–51. https://doi.org/10.1016/j.hcl.2011.10.002

Lixandrão ME, Ugrinowitsch C, Berton R et al (2018) The magnitude of muscle strength and mass adaptations between high-load resistance training versus low-load resistance training associated with blood-flow restriction: a systematic review and meta-analysis. Sports Med 48:361–378. https://doi.org/10.1007/s40279-017-0795-y

Loenneke JP, Fahs CA, Rossow LM et al (2013) Blood flow restriction pressure recommendations: a tale of two cuffs. Front Physiol 4:249. https://doi.org/10.3389/fphys.2013.00249

Long C, Conrad PW, Hall EA et al (1970) Intrinsic-extrinsic muscle control of the hand in power grip and precision handling: an electromyographic study. J Bone Joint Surg Am 52:853–867. https://doi.org/10.2106/00004623-197052050-00001

Lowe TW, Tenan MS, Shah K et al (2023) Low-load blood flow restriction reduces time-to-minimum single motor unit discharge rate. Exp Brain Res 241:2795–2805. https://doi.org/10.1007/s00221-023-06720-8

Madarshahian S, Letizi J, Latash ML (2021) Synergic control of a single muscle: the example of flexor digitorum superficialis. J Physiol 599:1261–1279. https://doi.org/10.1007/s00221-023-06720-8

McManus L, Hu X, Rymer WZ et al (2016) Fatigue increases beta-band coherence between the firing times of simultaneously active motor units in the first dorsal interosseous muscle. J Neurophysiol 115:2830–2839. https://doi.org/10.1152/jn.00097.2016

Nawab SH, Chang SS, De Luca CJ (2010) High-yield decomposition of surface EMG signals. Clin Neurophysiol 121:1602–1615. https://doi.org/10.1016/j.clinph.2009.11.092

Negro F, Farina D (2011) Linear transmission of cortical oscillations to the neural drive to muscles is mediated by common projections to populations of motoneurons in humans. J Physiol 589:629–637. https://doi.org/10.1113/jphysiol.2010.202473

Negro F, Farina D (2012) Factors influencing the estimates of correlation between motor unit activities in humans. PLoS ONE 7:e44894. https://doi.org/10.1371/journal.pone.0044894

Olmos AA, Montgomery TR Jr, Sears KN et al (2024a) Blood flow restriction increases necessary muscle excitation of the elbow flexors during a single high-load contraction. Eur J Appl Physiol 124(6):1807–1820. https://doi.org/10.1007/s00421-023-05405-y

Olmos AA, Montgomery TR, Sears KN et al (2024b) Blood flow restriction increases motor unit firing rates and input excitation of the biceps brachii during a moderate-load muscle action. J Sports Sci 42:1891–1903. https://doi.org/10.1080/02640414.2024.2413721

Pearson SJ, Hussain SR (2015) A review on the mechanisms of blood-flow restriction resistance training-induced muscle hypertrophy. Sports Med 45:187–200. https://doi.org/10.1007/s40279-014-0264-9

Peyrard A, Willis SJ, Place N et al (2019) Neuromuscular evaluation of arm-cycling repeated sprints under hypoxia and/or blood flow restriction. Eur J Appl Physiol 119:1533–1545. https://doi.org/10.1007/s00421-019-04143-4

Pope ZK, Willardson JM, Schoenfeld BJ (2013) Exercise and blood flow restriction. J Strength Cond Res 27:2914–2926. https://doi.org/10.1519/JSC.0b013e3182874721

Rossato J, Tucker K, Avrillon S et al (2022) Less common synaptic input between muscles from the same group allows for more flexible coordination strategies during a fatiguing task. J Neurophysiol 127:421–433. https://doi.org/10.1152/jn.00453.2021

Rossi FE, de Freitas MC, Zanchi NE et al (2018) The role of inflammation and immune cells in blood flow restriction training adaptation: a review. Front Physiol 9:1376. https://doi.org/10.3389/fphys.2018.01376

Singh RE, Iqbal K, White G et al (2018) A systematic review on muscle synergies: from building blocks of motor behavior to a neurorehabilitation tool. Appl Bionics Biomech. https://doi.org/10.1155/2018/3615368

Suga T, Okita K, Morita N et al (2009) Intramuscular metabolism during low-intensity resistance exercise with blood flow restriction. J Appl Physiol 106:1119–1124. https://doi.org/10.1152/japplphysiol.90368.2008

Watanabe T, Saito K, Ishida K et al (2018) Fatigue-induced decline in low-frequency common input to bilateral and unilateral plantar flexors during quiet standing. Neurosci Lett 686:193–197. https://doi.org/10.1016/j.neulet.2018.09.019

Windhorst U (2007) Muscle proprioceptive feedback and spinal networks. Brain Res Bull 73:155–202. https://doi.org/10.1016/j.brainresbull.2007.03.010

Wu CC, Lin YT, Hu CL et al (2024) Fatigue alleviation by low-level laser preexposure in ischemic neuromuscular electrical stimulation. Med Sci Sports Exerc 56:1795–1804. https://doi.org/10.1249/MSS.0000000000003472

Ye X, Beck TW, Wages NP (2014) Influences of dynamic exercise on force steadiness and common drive. J Musculoskelet Neuronal Interact 14:377–386

Zambolin F, Duro Ocana P, Goulding R et al (2024) The corticomuscular response to experimental pain via blood flow occlusion when applied to the ipsilateral and contralateral leg during an isometric force task. Psychophysiology 61:e14466. https://doi.org/10.1111/psyp.14466

Zijdewind I, de Groot MC, Kernell D (1998) Task-related variations in motoneuronal drive to a human intrinsic hand muscle. Neurosci Lett 242:139–142. https://doi.org/10.1016/s0304-3940(98)00049-4